Available online at www.sciencedirect.com

SCIENCE DIRECT®

Developmental Biology 270 (2004) 47–63

DEVELOPMENTAL BIOLOGY

www.elsevier.com/locate/ydbio

BMP receptor IA is required in the mammalian embryo for endodermal morphogenesis and ectodermal patterning

Shannon Davis,[a] Shigeto Miura,[b] Christin Hill,[a] Yuji Mishina,[b] and John Klingensmith[a,*]

[a] *Department of Cell Biology, Duke University Medical Center, Durham NC 27710, USA*

[b] *Laboratory of Reproductive and Developmental Toxicology, National Institute of Environmental Health Sciences, Research Triangle Park, NC 27709, USA*

Received for publication 16 September 2003, received 20 January 2004, accepted 27 January 2004

Available online 27 March 2004

Abstract

BMPRIA is a receptor for bone morphogenetic proteins with high affinity for BMP2 and BMP4. Mouse embryos lacking *Bmpr1a* fail to gastrulate, complicating studies on the requirements for BMP signaling in germ layer development. Recent work shows that BMP4 produced in extraembryonic tissues initiates gastrulation. Here we use a conditional allele of *Bmpr1a* to remove BMPRIA only in the epiblast, which gives rise to all embryonic tissues. Resulting embryos are mosaics composed primarily of cells homozygous null for *Bmpr1a*, interspersed with heterozygous cells. Although mesoderm and endoderm do not form in *Bmpr1a* null embryos, these tissues are present in the mosaics and are populated with mutant cells. Thus, BMPRIA signaling in the epiblast does not restrict cells to or from any of the germ layers. Cells lacking *Bmpr1a* also contribute to surface ectoderm; however, from the hindbrain forward, little surface ectoderm forms and the forebrain is enlarged and convoluted. Prechordal plate, early definitive endoderm, and anterior visceral endoderm appear to be expanded, likely due to defective morphogenesis. These data suggest that the enlarged forebrain is caused in part by increased exposure of the ectoderm to signaling sources that promote anterior neural fate. Our results reveal critical roles for BMP signaling in endodermal morphogenesis and ectodermal patterning.

Keywords: BMPRIA; BMP signaling; Epiblast; Mouse; Forebrain; Ectoderm; Endoderm; Anterior visceral endoderm

Introduction

Upon their formation at gastrulation, the primary germ layers must undergo regionalization and morphogenesis to establish the body plan. The mechanisms mediating these early processes remain obscure. However, they clearly depend on inductive interactions between the tissues of the early gastrula. In vertebrates, the origin of many of the cues for the initial regionalization of the germ layers is the gastrula organizer and its derivatives, including axial mesendoderm and prechordal plate (PrCP) (Harland and Gerhart, 1997; Shimamura and Rubenstein, 1997). In mammals, increasing evidence indicates that extraembryonic tissues also play a critical role in establishing the body plan. For instance, the anterior visceral endoderm (AVE) acts synergistically with the gastrula organizer to initiate development of the forebrain (Tam and Steiner, 1999).

Recent work indicates that BMP signals play many roles in the establishment of the vertebrate body plan, particularly signaling by BMP4 and BMP2. These closely related ligands utilize a common signal transduction cascade. In vertebrates, BMP2 and BMP4 have been shown to utilize either of two type I receptors, BMPRIA or BMPRIB, and a type II receptor, BMPRII (Massague and Chen, 2000; Miyazono et al., 2001). Upon ligand binding, the receptor complex initiates a signal transduction cascade. We will refer to this pathway as the BMP2/4 signaling pathway.

Each of the three germ layers appears to depend on BMP2/4 signaling for its early development. In the naive *Xenopus* ectoderm, BMP activity represses neural fate and promotes surface ectoderm development (Weinstein and Hemmati-Brivanlou, 1999). Additional evidence suggests that BMP2/4 signaling inhibits anterior neural gene expression (Glinka et al., 1997; Hartley et al., 2001). BMP2/4 signaling promotes the generation of neural crest cells at the neural–surface ectoderm boundary in chick and frog (Knecht and Bronner-Fraser, 2002; Mayor and Aybar, 2001). In the mesoderm, BMP2/4 signaling promotes ven-

* Corresponding author. Department of Cell Biology, Duke University Medical Center, Box 3709, Durham NC 27710. Fax: +1-919-684-5481.

E-mail address: kling@cellbio.duke.edu (J. Klingensmith).

0012-1606/$ - see front matter © 2004 Elsevier Inc. All rights reserved.
doi:10.1016/j.ydbio.2004.01.048

tral identity in nascent tissue and limits the spatial extent of organizer gene expression (Fainsod et al., 1994); later it induces a cardiac fate in intermediate mesoderm (Schultheiss et al., 1997). Finally, in endoderm, ectopic BMP2/4 signaling represses foregut markers, suggesting a role in anterior–posterior patterning of the endoderm (Tiso et al., 2002). Underscoring the importance of regulating BMP signals after gastrulation commences, mouse embryos lacking the BMP2/4 antagonists Chordin and Noggin show defects in all three embryonic axes (Bachiller et al., 2000). This implies that many developmental processes are sensitive to levels of BMP2/4 signaling upon establishment of the germ layers.

In mammals, a major obstacle in studying potential requirements for BMP2/4 signaling in germ layer development is the essential role it performs in initiating gastrulation itself. Mouse embryos lacking BMP4 (Winnier et al., 1995), BMPRIA (Mishina et al., 1995), or BMPRII (Beppu et al., 2000) exhibit a block to gastrulation, such that mesoderm does not form. However, both of these receptors are expressed ubiquitously in post-gastrulation embryos (Beppu et al., 2000; Dewulf et al., 1995) and are thus in place to mediate BMP signaling during germ layer development. *Bmpr1b* is not expressed in the gastrula (Dewulf et al., 1995), and mice lacking this gene show no early defects (Yi et al., 2000). Thus, BMPRIB is unlikely to play a major role in generating the body plan, whereas BMPRIA is probably a critical mediator of BMP2/4 signaling in this process.

We have used embryonic stem cell chimeras and tissue-specific gene ablations to determine the requirements for *Bmpr1a* in gastrulation and germ layer development. We find that it is required in extraembryonic tissues for primitive streak and mesoderm formation, but is required in the epiblast for patterning and morphogenesis of the mesoderm and its derivatives (S.M., S.D., J.K., and Y.M., manuscript in preparation). Here we focus on the roles of epiblast BMPRIA signaling in the development of the ectoderm and endoderm. We used a conditional null allele of *Bmpr1a* (Mishina et al., 2002) to create embryos in which extraembryonic tissues are wild type, but epiblast tissues are primarily composed of mutant cells. These embryos gastrulate to form all three germ layers, but exhibit severe problems in morphogenesis. The anterior neural ectoderm is dramatically enlarged and convoluted, particularly the forebrain, at the expense of surface ectoderm.

Materials and methods

Mice

Mox2-Cre heterozygotes (B6.129S4-*Meox2*$^{tm1(cre)Sor}$) (Tallquist and Soriano, 2000) were mated to *Bmpr1a* null heterozygotes (B6.129S7-*Bmpr1a*^{tm1Bhr}) (Mishina et al., 1995). *Mox2*$^{cre/+}$; *Bmpr1a*$^{null/+}$ progenies were mated to homozygotes for a conditional allele *Bmpr1a*^{flox} (129S7-*Bmpr1a*^{tm2Bhr}) (Mishina et al., 2002), resulting in the embryonic lethal genotype *Mox2*$^{cre/+}$; *Bmpr1a*$^{null/flox}$. Embryos were generated by timed matings (Hogan et al., 1994) and staged as described (Downs and Davies, 1993; Kaufman, 1992). Embryos and mice were genotyped by PCR (Mishina et al., 2002) using yolk sac DNA or tail DNA, respectively (Hogan et al., 1994). *R26R* (129S4-Gt(ROSA)*26Sor*^{tm1Sor}) (Soriano, 1999) was crossed into the *Bmpr1a*^{flox} line to produce mice of the genotype *Bmpr1a*$^{flox/flox}$; *R26R/R26R*. These were mated to *Mox2*$^{cre/+}$; *Bmpr1a* $^{null/+}$ mice to assay for recombination in wild-type and *Bmpr1a* mosaic embryos.

Gene expression, proliferation, and histological sectioning

Whole mount in situ hybridization was preformed as described previously (Belo et al., 1997). Probes used were *Ap2α* (Mitchell et al., 1991), *Foxa1*, *Foxa2* (Sasaki and Hogan, 1993), *Gbx2* (Wassarman et al., 1997), *Gsc* (Camus et al., 2000), *HesX1* (Thomas et al., 1995), *Krox20* (Swiatek and Gridley, 1993), *Cer1* (Pearce et al., 1999), *mDkk1* (Glinka et al., 1998), *Msx1* (Mackenzie et al., 1991), *Netrin-1* (Kennedy et al., 1994), *Noggin* (McMahon et al., 1998), *Otx2* (Ang et al., 1994), *Shh* (Echelard et al., 1993), *Six3* (Oliver et al., 1995), *Sox2* (Wood and Episkopou, 1999), *Sox10* (Kuhlbrodt et al., 1998), *T* (Wilkinson et al., 1990), *Wnt1* (Wilkinson et al., 1987), and *Wnt6* (Gavin et al., 1990). For AFP, a 906-bp fragment encoding exons 3–9 of AFP (a gift from SM Tilghman) was cloned into pBluescript (Stratagene). For two-probe in situ hybridization, embryos were concurrently incubated with one probe labeled with digoxigenin-UTP and a second probe labeled with fluorescein-UTP. The first staining reaction was performed in NBT/BCIP, after which the alkaline phosphatase was inhibited by a 5-min wash in 0.1 M Glycine, pH 2.2. The second color reaction was preformed using 350 μg/ml BCIP. Three or more mutant embryos were examined for each probe. For most tissues, patterning was assessed using multiple probes.

Expression *LacZ* from the *R26R* locus was detected by X-gal staining of embryos, followed by sectioning when necessary (Hogan et al., 1994). To quantify recombination, stained (recombined) cells and total cells were counted in a defined area of tissue over three near adjacent sections. Cell proliferation was assayed using an antibody against phosphorylated histone H3 (Upstate Biotechnology) as described previously (Anderson et al., 2002).

Area and density measurements

Eight adjacent sections from three different axial levels were used to measure the area of neural, mesoderm, and surface ectoderm in three wild-type and three *Bmpr1a*

mosaic embryos using NIH Image. Measurements were pooled at each axial level for a given tissue in each embryo. For mesoderm density, sections from two wild-type and two *Bmpr1a* mosaic embryos were stained with DAPI (Roche). The total number of cells in a defined area was determined from each of four sections in each embryo. Wild-type and mosaic numbers were compared using a paired T test.

Results

Ablation of Bmpr1a specifically in the epiblast

We designed an experimental approach to leave extra-embryonic activity intact while reducing BMPRIA signaling in embryonic tissues from before gastrulation. We used a gene-targeting strategy in which the receptor is ablated only in the epiblast. We employed a conditional null allele of *Bmpr1a* (Mishina et al., 2002) in which an essential exon is flanked by LoxP sites, the target sequences for Cre recombinase. *Mox2-Cre* (*MORE*) expression begins at E5.5, just before gastrulation, specifically in the epiblast (Tallquist and Soriano, 2000). Because the epiblast gives rise to all the cells of the embryo proper, this approach yields a conceptus deficient for *Bmpr1a* in embryonic tissues, but wild-type in extra-embryonic tissues, before germ layer formation.

In preparation for ablating *Bmpr1a* in the epiblast, we examined the recombination activity of *Mox2-Cre* in our experimental system. *Mox2-Cre* has been reported to be mosaic in activity in some studies (Hayashi et al., 2002) but not others (Wu et al., 2003). We crossed *Mox2-Cre* mice with mice carrying the *R26R* Cre reporter locus (Soriano, 1999), which expresses β-galactosidase (β-gal) in any cell in which Cre is active. At gastrulation through organogenesis stages (embryonic day (E)7.0–9.5), activity was observed in tissues of epiblast origin, but not in tissues of trophoblast origin (Figs. 1A and E). However, recombination was incomplete (Figs. 1B–D). Histological sections revealed the highest level of recombination was approximately 90% of cells (Fig. 1C). Most embryos are primarily composed of mutant cells: of 38 embryos assayed for recombination activity in whole-mount, 29 (76%) had well above 50% recombination. No specific tissue appeared to have a higher or lower degree of recombination, and labeled cells were distributed evenly among all tissues.

As an independent means of determining whether recombination by *Mox2-Cre* is sufficient to recombine all $Bmpr1a^{flox}$ alleles in epiblast derivatives, we used polymerase chain reaction to amplify recombined and unrecombined *Bmpr1a* conditional alleles in embryonic tissue from matings between *Mox2-Cre;* $Bmpr^{null}$ and $Bmpr1a^{flox/flox}$ parents. As expected, the recombined $Bmpr1a^{flox}$ allele was only found in embryos that carried Cre; however, all Cre-positive embryos carried both recombined and unrecombined $Bmpr1a^{flox}$ alleles (data not shown). In effect, then, *Mox2-Cre* enables us to produce mosaic embryos composed of mutant cells interspersed with wild-type (heterozygous) cells, while trophoblast-derived (extraembryonic) tissues remain wild type. We henceforth refer to these *Mox2-Cre;* $Bmpr1a^{flox/null}$ conceptuses as *Bmpr1a* mosaic embryos.

BMPRIA is required in the epiblast for multiple aspects of germ layer development

All embryos mosaic for *Bmpr1a* activity gastrulate and form a primitive streak, but exhibit severe and characteristic defects in the development of all three germ layers. Phenotypic mutants can be identified from E7.5 by their dysmorphic shape (Fig. 2C). The most conspicuous defect is that the anterior end is severely distorted, with an expanded, convoluted ectoderm (Fig. 2D). The posterior is less affected, and an allantois forms but never fuses with the chorion. Mosaic embryos fail to turn and maintain a cup-shaped appearance, surviving until E10.5–11.0 (Table 1). They form no heart and most likely die due to a lack of blood circulation (data not shown).

Given the variability of recombination from *Mox2-Cre*, we expected a wide range of phenotypes; however, we found that the defects were quite consistent. We scored embryos based on the appearance of the anterior end, the most variable aspect of the phenotype. The vast majority of mosaic embryos (92%; $n = 74$) had severe convolutions such that discrete headfolds could not be recognized (Fig. 3A). A few (6%; $n = 5$) had recognizable but highly dysmorphic headfolds (Fig. 3B). Very rarely (2%; $n = 2$), mosaics had symmetric headfolds, but like the other classes had stereotypic morphogenetic defects, including a failure in ventral closure (Fig. 3C).

We used the recombination reporter *R26R* to analyze recombination in *Bmpr1a* mosaic embryos. In these embryos, Mox2-Cre catalyzes recombination simultaneously of the $Bmpr1a^{flox}$ and *R26R loci*, in both cases leading to the deletion of a small segment of DNA. Surprisingly, embryos with widely different levels of recombination had remarkably similar phenotypes. Embryos with nearly 90% recombination looked very similar to embryos with less than 50%, and would be scored as the most severe phenotype (compare Figs. 3D–F). These results imply that BMPRIA signaling controls a cell non-autonomous mechanism of embryonic morphogenesis.

Cells lacking BMPRIA populate definitive endoderm, mesoderm, and ectoderm

We considered that the consistency of the mutant phenotype might be the result of mutant cells being disproportionately represented in a key tissue. If this tissue was in turn the source of inductive signals controlling the patterning or

growth of other tissues, one might expect to see a fairly consistent phenotype regardless of the overall degree of recombination. However, in examining many E7.0–8.5 mosaics in which mutant cells were marked, we found no specific tissue or structure that had overtly more or fewer mutant cells than other tissues in a given intact embryo. This

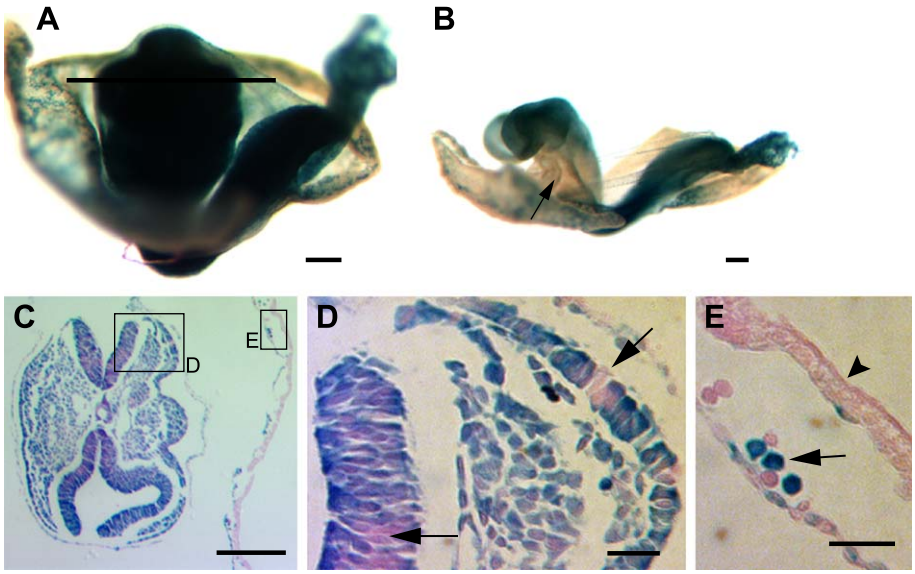

Fig. 1.

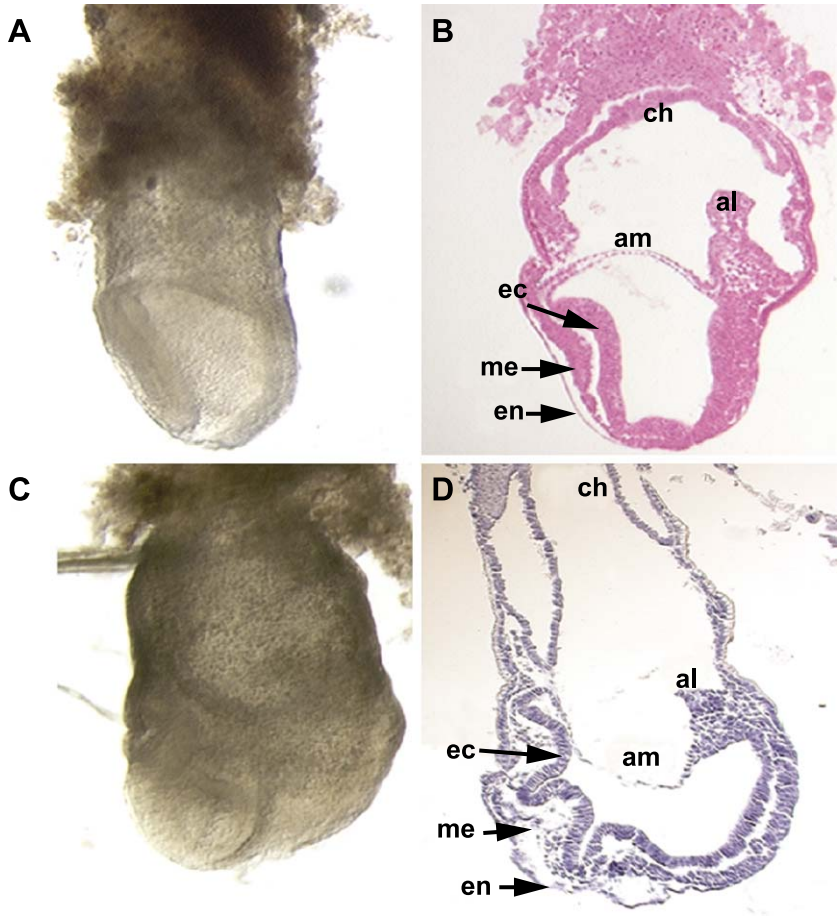

Fig. 2.

Table 1
Occurrence of *Bmpr1a* mosaic embryos at various embryonic stages

Age	Number of mutants	Total embryos	Percentage of mutant
E7.5	25	99	25
E8.5	116	493	24
E9.5	56	202	28
E10.5	8	54	15
E13.5	0	12	0
E14.5	0	8	0
E17.5	0	5	0
P0	0	15	0

Expected Mendelian ratios are observed before E10.5. After E10.5, *Bmpr1a* mosaic embryos are not recovered.

was the case regardless of whether the embryo had a relatively high or low level of recombined (mutant) cells. To investigate this further, we quantified recombined cells in a pair of sectioned embryos, *Bmpr1a* mosaic and wild-type, that both appeared to be about 50% chimeric based on the level of stained cells in whole-mount. The *Bmpr1a* mosaic had the characteristic "strong" phenotype shown in Figs. 3D–F. No specific tissue or germ layer had disproportionate levels of marked cells in either embryo (Figs. 3G and H; data not shown). Mutant cells contributed at normal levels to definitive endoderm and mesoderm, though these tissue layers do not form in *Bmpr1a* null homozygotes due to the lack of gastrulation (Mishina et al., 1995). Note that the endodermal layer in these mosaic embryos must be definitive endoderm-derived from the epiblast rather than trophoblast—because it contains labeled cells reflecting the epiblast-specific expression of *Mox2-Cre*. In short, BMPR1A signaling in the epiblast does not restrict cells to or from any of the germ layers or major tissues in the early embryo. This indicates that BMPRIA is not required for mesoderm or definitive endoderm cell identity or germ layer formation.

Ectodermal domains are abnormal in embryos mosaic for BMPRIA function

A striking defect of *Bmpr1a* mosaic embryos is that the anterior of the embryo appears enlarged, with a deeply convoluted ectodermal layer. To characterize the nature of ectodermal domains in mosaics, we assayed expression of neural and surface ectoderm markers. *Sox2* shows pan-neural expression in early mouse embryos (Wood and Episkopou, 1999), being expressed throughout the columnar epithelium of the neural tube (Figs. 4A–C). In *Bmpr1a* mosaics, the deep ectodermal folds at the anterior are composed of thick, columnar epithelium that expresses *Sox2* (Figs. 4D and E). Posterior sections have a discrete neural groove, though the *Sox2*-expressing columnar epithelium is not formed into a neural tube. This epithelium merges laterally with low, cuboidal tissue that does not label with *Sox2*, suggesting it is surface ectoderm (Fig. 4F). We conclude that the columnar epithelium in mosaics is neural ectoderm, relatively normal in morphology in the posterior but highly convoluted and broad in the anterior.

Surface ectoderm is labeled specifically by *Wnt6* expression (Gavin et al., 1990) and appears in wild-type embryos as thin epithelium adjoining the neural plate (Figs. 4G–I). Sections through the anterior of *Bmpr1a* mosaic embryos lack *Wnt6* expression in the ectoderm (though it is expressed in the amnion), consistent with the lack of thin, cuboidal epithelium in the anterior ectoderm (Figs. 4J and K). In contrast, posterior sections show *Wnt6* expression in the thin ectoderm lateral to the columnar neuroepithelium (Fig. 4L). Histological data also indicate that anterior sections have broad, thick (neural) ectoderm and little if any thin (surface) ectoderm (Fig. 4M), while posterior sections contain medial thick, columnar (neural) ectoderm flanked by thin (surface) ectoderm (Fig. 4N), as in wild type. Together, these results demonstrate that the anterior ectoderm of *Bmpr1a* mosaics is virtually all neural, while more caudal levels have both surface and neural ectoderm.

BMPRIA is required for anterior surface ectoderm but not for the surface ectoderm fate

Recent work in *Xenopus* suggests naive ectodermal cells that undergo little BMP2/4 signaling are unable to become surface ectoderm and become neural by default (Weinstein

Fig. 1. Tissue distribution of Mox2-Cre activity. Recombined cells are marked by β-galactosidase staining, demonstrating recombination at the *R26R* reporter locus. (A–B) Wild-type E8.25 embryos, lateral view. (A) Although this embryo appears to be entirely marked in whole-mount view, sections reveal significant unrecombined cells. The extraembryonic yolk-sac shows much less staining because all but the yolk-sac mesoderm is of trophoblast origin. Line indicates level of section in panel C. (B) This embryo exhibits a much lower level of recombination, with a region of few marked cells (arrow). (C) Transverse, eosin-counterstained section through A. Note unlabeled (pink) cells in all tissues. Inset boxes show areas shown in panels D and E. (D) Arrows indicate examples of unrecombined (pink) cells in ectodermal domains. (E) Extraembryonic tissues exhibit both recombined (blue) and unrecombined (pink) cells in epiblast derivatives (arrowhead), but only unrecombined cells in trophoblast derivatives (arrowhead). Scale bars = 0.25 mm, except D and E = 0.025 mm.

Fig. 2. Morphological defects of *Bmpr1a* mosaic embryos at the end of gastrulation. In all panels, anterior is the left, posterior is to the right, and proximal is up. (A) Wild-type E7.5 embryo, lateral view. (B) Sagittal section of the embryo shown in panel A. Extraembryonic structures include the chorion (ch), the amnion (am), and the allantois (al). In the embryo proper, the embryonic ectoderm (ec), mesoderm (me), and endoderm (en) layers are indicated. (C) *Bmpr1a* mosaic embryo at E7.5. It has a broader, shorter profile than wild-type. (D) Sagittal section of the embryo shown in panel C. Extraembryonic structures are present, including the allantois, amnion, and chorion. The most conspicuous defect is that the embryonic ectoderm is highly convoluted, particularly in the anterior portion of the embryo. The anterior mesoderm appears less organized.

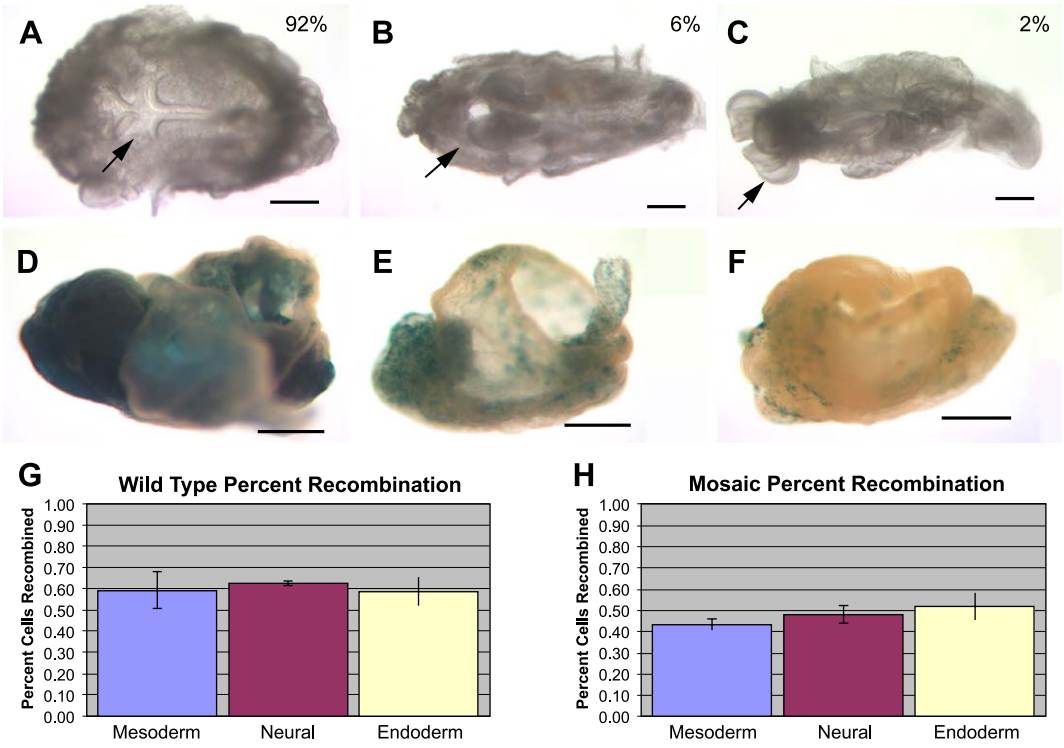

Fig. 3. Spectrum of phenotypes and recombination in *Bmpr1a* mosaic embryos. (A) 91% of *Bmpr1a* mosaic embryos have severe distortions of the anterior end (arrow). (B) 6% of *Bmpr1a* mosaic embryos have recognizable headfolds (arrow), although these structures are severely distorted. (C) 3% of *Bmpr1a* mosaic embryos have symmetrical headfolds (arrow), but have a failure in ventral morphogenesis and other defects that characterize all *Bmpr1a* mosaics. (D–F) *Bmpr1a* mosaic E8.5 embryos with varying degrees of recombination at the *R26R* reporter locus. Phenotypes are virtually identical through the levels of recombination vary from approximately 90% (D) to less than 50% (F). (G and H) Quantitation of recombination in tissues of wild-type and mutant mosaic embryos that appeared about 50% recombined at the *R26R* locus in whole-mount. (G) Percentage of recombined cells in a $Mox2^{cre/+}$; $Rosa^{R26R/+}$ (wild-type) embryo in embryonic mesoderm, neural ectoderm, and embryonic endoderm. (H) Levels of recombination in a $Mox2^{cre/+}$; $Bmpr1a^{flox/null}$; $Rosa^{R26R/+}$ embryo in same three tissues. Error bars are ±SEM. Scale bars = 0.5 mm.

and Hemmati-Brivanlou, 1999). Although we observed caudal surface ectoderm in *Bmpr1a* mosaics, the chimeric nature of these embryos raises the possibility that this tissue is entirely wild type, that is, it is possible that *Bmpr1a* null cells are unable to participate in the formation of surface ectoderm. Using *R26R* as a reporter of recombination in *Bmpr1a* mosaic embryos, we assessed the genotypic composition of the surface ectoderm. We saw no exclusion or abnormal contribution of recombined cells in the surface ectoderm (Figs. 4P and Q); moreover, the distributions of recombined cells were similar between surface and neural ectoderm domains, and were consistent with distributions in other germ layers (see also Figs. 3G and H). Thus, despite the paucity of anterior surface ectoderm in *Bmpr1a* mosaics, these data indicate that *Bmpr1a* is not required for surface ectoderm cell fate per se.

Precursor tissues of the head are enlarged in Bmpr1a mosaic embryos

The convolutions of the anterior neural epithelium in mosaic embryos could result from an expansion of neural tissue; however, they might also be explained by a deficiency in head mesenchyme, which could cause the overlying neural epithelium to wrinkle without the support of underlying mesoderm. Given that molecular marker analysis confirmed that the thick, columnar ectoderm is indeed neural, and that the contiguous cuboidal epithelium is surface ectoderm, we used histology to identify tissues and determined their surface area in serial sections. Relative to wild-type tissues, the anterior neurectoderm of mosaic embryos is indeed expanded, and there is a corresponding expansion of underlying mesenchyme (Fig. 4O). The density of mesoderm cells did not differ significantly between wild-type and mosaic embryos (P value = 0.35).

The enlarged neurectoderm of *Bmpr1a* mosaics could result from a conversion of surface to neural ectoderm fates, or from an over-proliferation of neural cells. We determined the proliferating cells per unit area of neural tissue in *Bmpr1a* mosaic and wild-type embryos. The number of proliferating cells in the anterior ectoderm was not significantly different between *Bmpr1a* mosaic and wild-type embryos (P value = 0.68). Overall, our data suggest that the expanded neural domain results from a conversion of surface to neural ectoderm fate specifically in the anterior of the embryo.

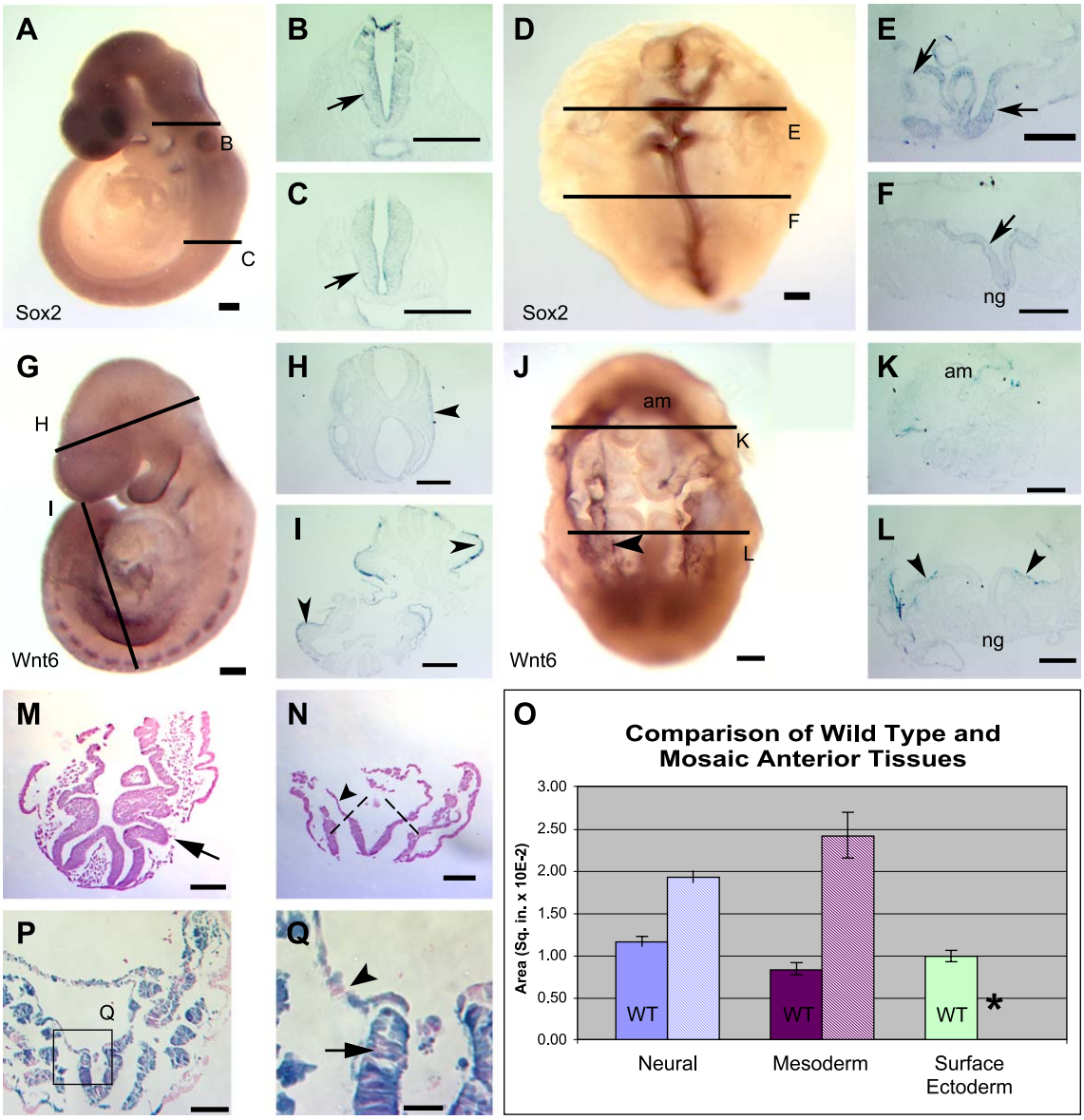

Fig. 4. Distribution of neural and surface ectoderm in *Bmpr1a* mosaics. (A–F) *Sox2* whole-mount in situ hybridization and derivative histological sections. (A) Wild-type, E9.5 embryo, lateral view. *Sox2* expression occurs throughout the neural tube. Transverse lines show level of sections in panels B and C. (B and C) Expression of *Sox2* is observed only in neural ectoderm (arrows) at both axial levels. (D) *Bmpr1a* mosaic E9.5 embryo, ventral view. Levels of sections shown in E and F indicated by lines. (E) In rostral sections of *Bmpr1a* mosaic embryos, *Sox2* expression occurs throughout the columnar ectodermal epithelium, which is highly convoluted and extends to the margins of the embryo (arrows). Expression is highest medially and tapers to lower levels laterally. (F) In trunk-level sections, *Sox2* expression occurs in the columnar epithelium (arrow); a discrete neural groove (ng) is formed and the columnar epithelium is flanked by low cuboidal epithelium that does not express *Sox2*. (G–L) *Wnt6* in situ hybridization of wild-type and *Bmpr1a* mosaic embryos. (G) Wild-type E9.5 embryo, lateral view. *Wnt6* is expressed in surface ectoderm. (H and I) Transverse sections of wild-type embryo hybridized with *Wnt6* probe. Surface ectoderm specifically expresses *Wnt6* (arrowheads), while neural ectoderm does not express *Wnt6*. (J) *Bmpr1a* mosaic, E9.5 embryo, dorsal view. *Wnt6* expression in the amnion (am) occurs as a dark ring at the lateral margins of the embryo. Surface ectoderm expression of *Wnt6* is seen caudally (arrowhead). (K) Rostral sections of mutants show no clear *Wnt6* expression in ectoderm, only amnion expression (am). (L) Caudally, *Wnt6* is expressed in surface ectoderm (arrowheads) lateral to the thickened medial (neural) ectoderm. (M and N) Eosin-stained transverse sections of E8.5 *Bmpr1a* mosaic embryo. (M) Rostral section reveals highly convoluted neural epithelium (arrow), with no histologically detectable surface ectoderm. (N) Trunk section reveals surface ectoderm (arrowhead) lateral to neural epithelium. Dashed lines indicate transition from neural to surface ectoderm. (O) Area of anterior tissues in wild-type and *Bmpr1a* mosaic embryos (E8.0). For each tissue, solid colored bars (left) represent wild-type embryos, and stippled bars (right) represent mosaic embryos. *P* values are neural = 1.1×10^{-8}, mesoderm = 2.4×10^{-7}. Asterisk represents that no morphological evidence for anterior surface ectoderm was observed for *Bmpr1a* mosaic embryos. Error bars are ± SEM. (P) X-gal and eosin-stained transverse trunk section of $Mox2^{cre/+}$; $Bmpr1a^{flox/null}$; $Rosa^{R26R/+}$ embryo. (Q) Higher magnification view of P as indicated. Unrecombined (pink, wild-type) cells are intermingled with recombined (blue, mutant) cells in both neural (arrow) and surface (arrowhead) ectoderm. Scale bars = 0.25 mm, except Q = 0.025 mm.

Anterior–posterior patterning of the neural plate in Bmpr1a mosaic embryos

To determine the anterior–posterior (A–P) axial level at which the neuroepithelium becomes expanded, we examined several regionally restricted gene expression markers. At E7.5, the boundary between *Otx2* and *Gbx2* expression (Fig. 5A) defines the posterior extent of the midbrain (Wassarman et al., 1997). As in wild-type embryos, the caudal aspect of the *Gbx2* expression domain in mutants extends to the posterior primitive streak. In contrast, mosaic embryos show a greatly enlarged domain of *Otx2* compared to stage-matched wild-type control embryos; a clear boundary forms, but it is shifted toward the tail end of the embryo (Fig. 5B). This indicates that the presumptive brain is enlarged from early stages.

To further define the A–P axis in *Bmpr1a* mosaic embryos, we examined regional neural markers at E8.0. *Krox20* expression marks rhombomeres 3 and 5 (r3 and 5) in the hindbrain (Fig. 5C) (Swiatek and Gridley, 1993). Though sometimes obscured by anterior convolutions, both the r3 and r5 stripes occur in mosaics (Fig. 5D). Caudal to the r5 stripe, the ectoderm appears relatively normal, suggesting that the neural epithelium is expanded from the rostral hindbrain through its anterior limit. We also noticed that the space between the r3 and r5 stripes sometimes appears compressed. A similar result was obtained with the midbrain marker *Wnt1* (Wilkinson et al., 1987); a much narrower band was observed in mutant embryos relative to wild-type littermates (Figs. 5E and F). In contrast, expression of *Six3*, which marks the early forebrain, is expanded in mosaics compared to wild type (Figs. 5G and H). Intriguingly, sometimes the most rostral portion of the anterior neural ectoderm showed less intense staining for forebrain markers than tissue immediately caudal; we believe this reflects an underlying prechordal plate defect (see below). Taken together, our results demonstrate that A–P patterning occurs in the neural ectoderm of *Bmpr1a* mosaic embryos. A convoluted, broad neural epithelium extends from the caudal hindbrain forward to the rostral end of the embryo. Most of this tissue appears to be of forebrain character, possibly at the expense of the midbrain and hindbrain.

Dorsal–ventral patterning of the neural plate in Bmpr1a mosaic embryos

Embryological manipulations and genetic analysis in zebrafish, *Xenopus*, and chick suggest that BMP2/4 signaling has a major role in dorsal–ventral (D–V) patterning of the body plan, including the ectoderm (Lee and Jessell, 1999). We examined D–V patterning in *Bmpr1a* mosaics to elucidate the role of BMP2/4 signal transduction during this process in mouse. Surprisingly, even in very strong mosaics, the ventral neural tube marker *Netrin-1* (Kennedy et al., 1994) is expressed in domains similarly delimited as in wild type (Figs. 6A–E). Where the large convolutions of the expanded anterior neural plate approach the midline, multiple domains of *Netrin-1* expression occur (Fig. 6D). These data complement and support similar results with *Shh*

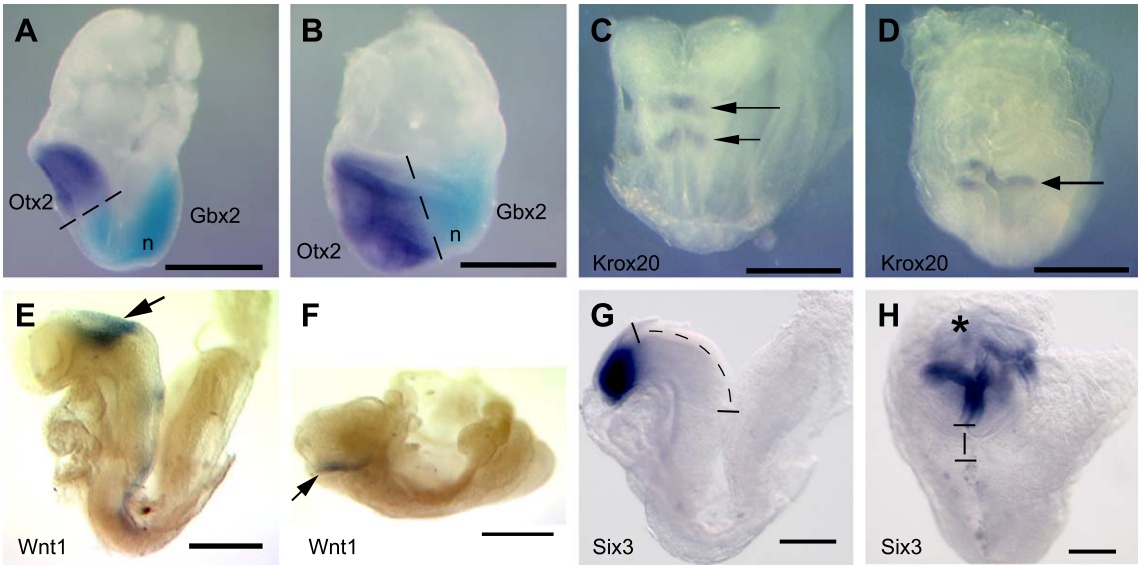

Fig. 5. Expansion of anterior tissues in *Bmpr1a* mosaics. (A–B) *Otx2* (purple) and *Gbx2* (light blue) in situ hybridization. Dashed line indicates mid–hindbrain boundary, n indicates node. (A) Wild-type E7.5 embryo, lateral view (B) *Bmpr1a* mosaic E7.5 embryo, lateral view. (C–D) *Krox20* in situ hybridization as indicated by arrows. (C) Wild-type E8.5 embryo, dorsal view. (D) *Bmpr1a* mosaic E8.5 embryo, ventral view. (E–F) *Wnt1* in situ hybridization as indicated by arrows. (E) Wild-type E8.5 embryo, lateral view. (F) *Bmpr1a* mosaic E8.5 embryo, lateral view. (G–H) *Six3* in situ hybridization. Dashed lines represent distance between *Six3* expression and the hindbrain. (G) Wild-type E8.5, lateral view. (H) *Bmpr1a* mosaic embryo, ventral view. Scale bars = 0.5 mm.

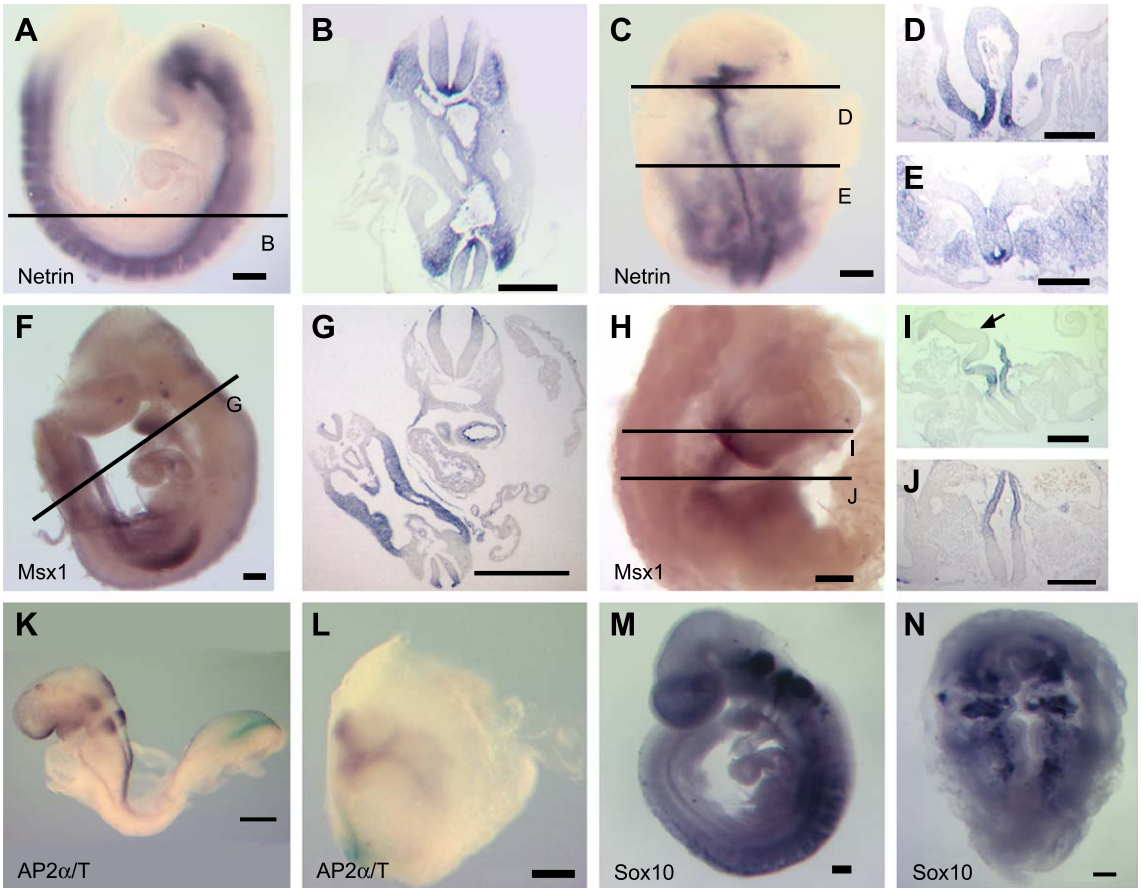

Fig. 6. Dorsal–ventral patterning of the neural tube. (A–E) *Netrin* in situ hybridization. (A) Wild-type E9.5 embryo, lateral view. (B) Transverse section of embryo in A at level indicated. (C) *Bmpr1a* mosaic E9.5 embryo, ventral view. (D) Transverse section of embryo in C at level indicated. (E) Transverse section of embryo in C at level indicated. (F–J) *Msx1* in situ hybridization. (F) Wild-type E9.5 embryo, lateral view. (G) Transverse section through F at level indicated. (H) *Bmpr1a* mosaic E9.5 embryo, dorsal view. (I and J) Transverse section of embryo in H at levels indicated. Arrow in I indicates lateral neuroectoderm with no *Msx1* staining. (K and L) *Ap2*α (purple) and *T* (light blue) in situ hybridization. (K) Wild-type E8.5 embryo, lateral view. (L) *Bmpr1a* mosaic E8.5 embryo, lateral view. (M and N) *Sox 10* in situ hybridization. (M) Wild-type E9.5 embryo, lateral view. (N) *Bmpr1a* mosaic E9.5 embryo, ventral view. Scale bars = 0.25 mm.

expression (see below), and suggest that the regulation of ventralizing pathways is largely unperturbed in these embryos. Dorsal neural markers, such as *Msx1* and *Pax3*, are expressed in dorsal domains in the caudal neural tube and are sometimes expanded (Figs. 6F–K; data not shown). In the convoluted, anterior regions devoid of surface ectoderm, expression of these dorsal markers occurs in regions of the neurectoderm away from the ventral midline, but not uniformly in such regions (Fig. 6I).

We further characterized D–V ectodermal patterning by evaluating neural crest markers. *AP2α* is an early marker of the neural crest competence domain (Mitchell et al., 1991) and is expressed in mosaic embryos (Figs. 6K and L). The migratory neural crest cell marker *Sox10* (Kuhlbrodt et al., 1998) is expressed in *Bmpr1a* mosaics in cells located peripheral to the neural tube, very similar to the pattern observed in wild type (Figs. 6M and N). Thus, despite the severe morphological defects of the neural epithelium in these BMPRIA-deficient embryos, dorsal fates do not appear to be reduced nor ventral fates increased.

Anterior axial mesendoderm is expanded in BMPRIA mosaics

To explore the basis for the expanded anterior neural epithelium in *Bmpr1a* mosaic embryos, we assessed the status of tissues known to influence the early development of the ectoderm. Axial patterning is conferred in part by the underlying mesendoderm, which derives from the organizer (Harland and Gerhart, 1997). We used several markers for the node and axial midline to examine the nature of axial tissue in *Bmpr1a* mosaic embryos. The primitive streak, node, and notochord are all present (Fig. 7A). The axial midline is always shorter, and the node and axial mesendoderm are usually somewhat broader during early somitogenesis (Figs. 7B and C). This is especially pronounced at the anterior end of the mesendoderm, which typically appears broad and diffuse.

The rostral-most axial mesendoderm is the prechordal plate, which has a key role in patterning the overlying ventral neural epithelium of the presumptive forebrain

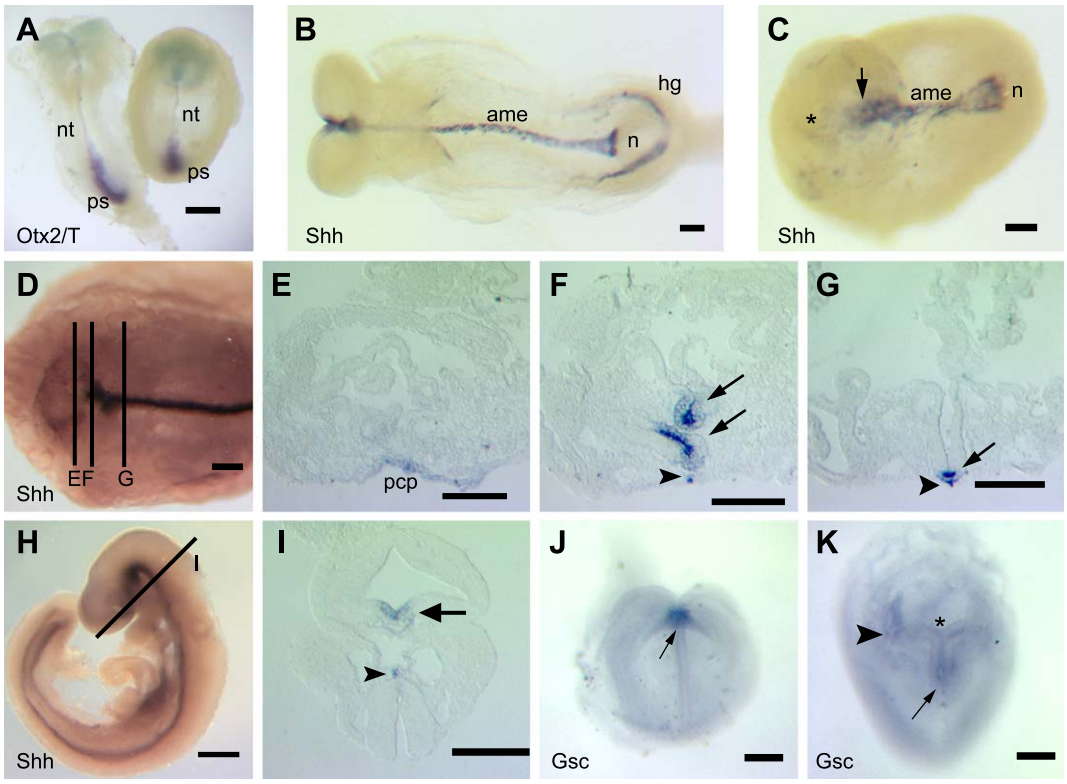

Fig. 7. Axial tissues in *Bmpr1a* mosaics. (A) A pair of E8.5 littermates, wild-type on left and mosaic on right, showing *Otx2* (light blue) and *T* (purple) in situ hybridization. nt = notochord, ps = primitive streak (B–I) *Shh* in situ hybridization. (B) Wild-type E8.5 embryo, ventral view. (C) *Bmpr1a* mosaic E8.5 embryo, ventral view. Arrow indicates intense rostral staining. Asterisk indicates tissue anterior to *Shh* expression. For B and C: ame, axial mesendoerm; hg, hindgut; n, node. (D) *Bmpr1a* mosaic E9.5 embryo, ventral view. (E–G) Transverse sections of embryo in D at levels indicated. Arrow indicates floor plate expression, arrowheads indicate notochord expression. PCP, prechordal plate. (H) Wild-type E9.5 embryo, lateral view. (I) Transverse section of embryo in H at level indicated. Arrow indicates prechordal plate and arrowhead indicates notochord. (J and K) In situ hybridization for *Gsc*. (J) Wild-type E7.5 embryo, anterior view. Arrow indicates prechordal plate staining. (K) *Bmpr1a* mosaic E7.5 embryo, ventral view. Arrow indicates midline, prechordal plate expression and arrowhead indicates an ectopic focus of expression. Asterisk indicates tissue anterior to *Gsc* expression. Scale bars = 0.25 mm.

(Anderson et al., 2002; Shimamura and Rubenstein, 1997). *Shh* is expressed in prechordal plate, as well as in the floor plate of the ventral neural tube, the notochord, and the ventral endoderm of the closing foregut and hindgut (Figs. 7B, H, and I). In mosaic embryos, *Shh* expression typically appears more diffuse and expanded laterally at anterior levels (Figs. 7C and D). Histological sections of such embryos reveal a broad domain of labeled mesendoderm underlying the anterior neural plate, suggesting an expansion of the prechordal plate (Fig. 7E). In the convoluted anterior, multiple bends of the neural epithelium express *Shh* adjacent to the notochord (Fig. 7F), while at posterior levels the normal pattern of axial midline expression is observed (Fig. 7G). This suggests that floorplate identity is induced in multiple anterior locations where bends in the neural ectoderm approach the notochord. Note, however, that despite the analysis of several markers of axial mesendoderm over dozens of mosaic embryos, we never saw a duplicated or partially duplicated axis.

We further examined the state of prechordal plate using the markers *Goosecoid* (*Gsc*) and *Dickkopf1* (*Dkk1*), which mark this tissue specifically (Camus et al., 2000; Glinka et al., 1998). Relative to wild-type littermates (Fig. 7J), mosaic embryos have diffuse, broad domains of *Gsc* and *Dkk1* expression (Fig. 7K; data not shown). However, prechordal plate markers usually fail to extend to the rostral limit of the midline as in wild-type embryos (Figs. 7B vs. C); thus, there is often a portion of apparent neural epithelium that is anterior to the axial mesendoderm in *Bmpr1a* mosaics (asterisks in Figs. 7C and K). Note that this same domain often expresses forebrain markers less intensely than tissues immediately to the posterior (Fig. 5F), which likely overlie the broad prechordal plate. Thus, the axial mesendoderm in *Bmpr1a* mosaics is often somewhat broadened but nevertheless quite discrete at trunk levels; moreover, it is active as an inductive signaling source, as judged by its ability to induce floor plate character in adjacent neural epithelium. At the anterior end of the midline mesendoderm, however, the prechordal plate is expanded and diffuse, underlying an enlarged portion of the anterior neural plate.

Abnormal distribution of definitive endoderm and anterior visceral endoderm

The broad prechordal plate in *Bmpr1a* mosaic embryos raises the issue of endodermal development in these

mutants, in that the mouse prechordal plate coincides with the dorsal midline of the foregut endoderm (Shimamura and Rubenstein, 1997; Sulik et al., 1994). Moreover, the ventral hindgut domain of *Shh* is missing in mutant embryos (Figs. 7B and C). We examined the general state of endoderm using *Foxa1* as a marker (Figs. 8A–D), which is expressed in the endodermal gut tube as well as the overlying notochord and floor plate (Sasaki and Hogan, 1993). *Foxa1* is expressed throughout the ventral surface of *Bmpr1a* mosaic embryos (Fig. 8C). Histological sections demonstrate that the endoderm covers the ventral surface of these embryos, with no formation of a gut tube (Fig. 8D). Our analysis of the distribution of recombined cells in mosaic embryos (Fig. 3H) indicates that this tissue is definitive endoderm (derived from the epiblast). Even in the 2% of mosaics that form symmetric headfolds, the morphogenetic movements required to bring the lateral edges of the endoderm together do not occur and cause a failure in gut formation (Fig. 3C; data not shown). Thus, there is a general failure of endodermal morphogenesis in *Bmpr1a* mosaics; moreover, specific domains of the endoderm are abnormal, such as the expanded prechordal plate.

To analyze the initial stages of endoderm formation, we assessed markers for the early definitive endoderm and the visceral endoderm. Initially, the epiblast is covered by visceral endoderm; during gastrulation, it is replaced by

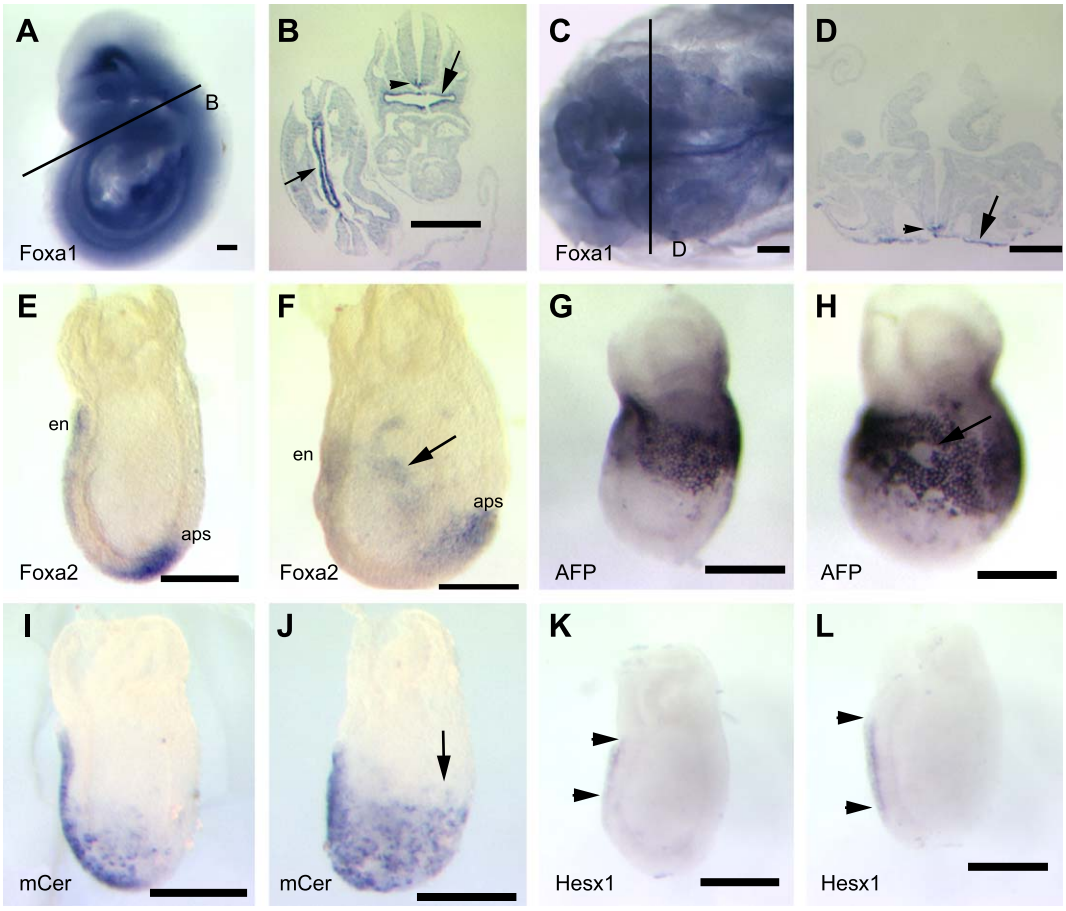

Fig. 8. Analysis of endoderm via in situ hybridization in *Bmpr1a* mosaics. (A–D) *Foxa1* in situ hybridization. (A) Wild-type E9.5 embryo, lateral view. The plane of section shown in panel B is indicated by the line. (B) Transverse section of wild-type embryo reveals strong expression of *Foxa1* throughout the endodermal gut tube (arrows). Floorplate or notochord expression is indicated by an arrowhead. (C) *Bmpr1a* mosaic E9.5 embryo, ventral view. The plane of section shown in panel D is indicated by the line. (D) Transverse section of mosaic embryo shows *Foxa1* expression throughout the ventral cell layer, illustrating that endoderm is present but fails to form a gut tube. Floorplate or notochordal expression is also present (arrowhead). (E) *Foxa2* probe in wild-type E6.75 (late-streak stage) embryo, lateral view, shows anterior primitive streak (aps) and anterior endoderm expression (en). This is most likely AVE expression because it is discontinuous with the anterior streak expression domain. However, the definitive endoderm from the anterior streak is beginning to form at this time, which also expresses *Foxa2*. (F) *Foxa2* expression in *Bmpr1a* mosaic E6.75 (late-streak) embryo, lateral view. Arrow indicates patchy ectopic expression in lateral region. (G) *AFP* expression in wild-type E7.0 embryo, lateral view, marking visceral endoderm. (H) *AFP* expression in *Bmpr1a* mosaic E7.0 embryo, lateral view. Arrow indicates lateral endodermal patches devoid of AFP staining. (I) *mCer1* expression in wild-type E7.0 embryo, lateral view. Distal expression is in newly forming definitive endoderm. (J) *mCer1* expression in *Bmpr1a* mosaic E7.0 embryo, lateral view. Arrow indicates ectopic, posterior expression in definitive endoderm. (K) *Hesx1* expression in wild-type E7.0 embryo, lateral view. Expression occurs in the AVE; arrowheads show boundaries of expression domain. (L) *Hesx1* expression in *Bmpr1a* mosaic E7.0 embryo. The extent of the AVE is increased, extending more distally than in wild type (compare distance between arrowheads in L and K). Scale bars = 0.25 mm.

definitive endoderm, most of which arises from the anterior primitive streak (Dufort et al., 1998; Lawson et al., 1991). The visceral endoderm is thus displaced proximally such that it no longer overlies the epiblast. The anterior visceral endoderm (AVE) transiently overlies the portion of the epiblast that gives rise to the brain (Quinlan et al., 1995); many lines of evidence suggest that the AVE has an important role in promoting forebrain development (Beddington and Robertson, 1998). At gastrulation, *Foxa2* is expressed in the AVE as well as in anterior primitive streak and the axial mesendodermal cells that emanate from it (Fig. 8E) (Sasaki and Hogan, 1993). In *Bmpr1a* mosaics, *Foxa2* expression occurs in these domains, though each is broader and less distinct; in addition, ectopic patches of expression often appeared on the lateral surfaces of these embryos (Fig. 8F). These patches are very likely ectopic definitive endodermal precursors because they did not express markers specific to the AVE (see below) or axial mesoderm. Further evidence suggesting abnormal morphogenesis of the early endoderm is the expression pattern of the *alpha-foetoprotein* (*AFP*) gene, a marker for extraembryonic visceral endoderm (Waldrip et al., 1998). In *Bmpr1a* mosaics, *AFP* was expressed in an uneven, patchy pattern in mutant embryos (Fig. 8H) relative to wild-type siblings (Fig. 8G). It is noteworthy that patches devoid of AFP expression (and thus visceral endoderm) were similar in distribution and size to the patches of ectopic *Foxa2* expression (probable definitive endoderm). These data suggest an abnormal distribution of visceral and definitive endoderm during gastrulation, and perhaps an intermingling of these tissues during gastrulation.

To further investigate the nature of the early endoderm in *Bmpr1a* mosaics, we assessed expression of several additional markers. Mouse *Cerberus-1* (*mCer1*) is expressed initially in the AVE but then transiently in the newly formed definitive endoderm as it displaces visceral endoderm (Pearce et al., 1999). Relative to wild type (Fig. 8I), *mCer1* expression in the definitive endoderm not only occurred in its normal domain but also extended more to the posterior than in wild type (Fig. 8J). Consistently, markers of the AVE, such as *Hesx1* (Thomas et al., 1995), were properly restricted to the anterior midline but exhibited an expanded domain that extended distally toward the anterior primitive streak (Figs. 8K and L). This suggests that AVE is abnormally displaced by the definitive endoderm. Together, these results indicate that early endoderm morphogenesis is abnormal in *Bmpr1a* mosaics, with abnormal exposure of the underlying ectoderm to patterning signals that may emanate from different regions of the endoderm.

Discussion

By ablating BMPRIA specifically in epiblast cells, we have circumvented the gastrulation block of *Bmpr1a* null embryos to reveal the roles of BMP2/4 signaling in the development of germ layers. All three germ layers form, and marked cells lacking *Bmpr1a* contribute to each at levels comparable to wild-type marked cells. Thus, BMPRIA is dispensable for endoderm and mesoderm formation despite their absence in *Bmpr1a* null embryos. However, each germ layer is abnormal; in this report, we focus on endoderm and ectoderm. Although mutant cells are able to contribute to surface ectoderm, little if any forms in the anterior of mosaic embryos. Rather, the prospective forebrain is greatly expanded and convoluted. Morphogenesis of both visceral and definitive endoderm is abnormal, such that domains known to promote anterior neurectoderm are expanded during the early patterning of the ectoderm.

The identity of BMP ligands that signal through BMPRIA to mediate this morphogenesis and patterning is unclear. *Bmp4* and *Bmpr1a* have essentially identical null phenotypes (Mishina et al., 1995; Winnier et al., 1995). Nonetheless, the defects we observe are unlikely to reflect unique requirements for BMP4 signaling in the epiblast, because its loss specifically in the epiblast has relatively mild defects (Fujiwara et al., 2002). In *Xenopus*, BMP2, BMP7 can repress neural and promote surface ectoderm fate (Suzuki et al., 1997). Nevertheless, in mouse, neither *Bmp2* nor *Bmp7* is expressed in a way that can account for the defects, nor is either uniquely required for any of the processes affected in the *Bmpr1a* mosaics (Zhao, 2003). The double and triple null embryos have yet to be generated to assess potential redundancy. It also remains possible that an unsuspected BMP is key.

Similarities and differences with zebrafish BMP pathway mutants

The phenotypes of mouse *Bmpr1a* epiblast mosaic embryos resemble those of zebrafish loss-of-function mutants for BMP pathway components, though there are some notable differences. The mouse phenotypes we observed are most comparable to the stronger phenotypes observed for mutants in *Bmp2b (swirl)*, *Bmp7* (*snailhouse*), and their signal transducer *Smad5* (*somitabun*) (Mullins et al., 1996; reviewed by Hammerschmidt and Mullins, 2002). Lack of both maternal and zygotic function of the TGFβ type I receptor *lost-a-fin* results in a very similar phenotype (Mintzer et al., 2001). In all these zebrafish mutants, the axial mesendoderm, derived from the organizer, exhibits a moderate lateral expansion, while the neural ectoderm is expanded at the expense of nonneural ectoderm. There are also similarities in dorsoventral neural patterning (discussed below). As in the fish mutants, the somitic mesoderm is expanded and the lateral mesoderm reduced in *Bmpr1a* epiblast mosaics (S.M., S.D., J.K. and Y.M., in preparation).

However, whereas we observed more severe defects in the anterior of *Bmpr1a* mosaic mouse embryos, the zebrafish defects are strong posteriorly and rather mild in anterior regions. For example, the head structures are comparatively normal, and there is no apparent broadening of the expres-

sion domain of markers for the most anterior axial mesendoderm, the prechordal plate (Mullins et al., 1996; Mintzer et al., 2001). In contrast, rostral structures are extremely dysmorphic and convoluted in *Bmpr1a* mosaics, with broad, diffuse staining of prechordal plate markers, while the trunk is much less affected (though neurulation fails at all axial levels). These differences are likely due in part to very different morphological constraints confronting the two types of embryo, such as the large yolk of the fish egg or the cupped shape of the mouse gastrula.

BMPRIA and morphogenesis of the mammalian embryo

Despite wide variability of *Mox2-Cre* recombination in *Bmpr1a* mosaic embryos, over 90% displayed a characteristic "strong" phenotype of a severely malformed anterior, and all mosaics had profound and consistent morphogenesis defects. The strong phenotype was observed in both low and high percentage mosaics. Moreover, mutant cells were evenly represented in all tissue layers and structures analyzed. These results indicate that the morphogenesis defects of BMPRIA inactivity are largely cell nonautonomous.

All *Bmpr1a* mosaic embryos displayed a lack of ventral closure and embryonic turning. These processes are developmentally coupled, though the causative cellular and molecular mechanisms are poorly understood (Kaufman and Bard, 1999). Furin is a protease involved in the maturation of growth factors, including BMP4 (Constam and Robertson, 2000), and is required in the definitive endoderm for both ventral closure and turning (Constam and Robertson, 2000). Embryos lacking *Smad5*, encoding a BMPRIA signal transducer, also show defective ventral closure and embryonic turning (Chang et al., 1999). Collectively, these results suggest that BMP signaling, acting through BMPRIA, is required for the coordinate regulation of these morphogenetic processes.

We also observed abnormal early endodermal morphogenesis in *Bmpr1a* mosaic embryos. During gastrulation, the definitive endoderm (DE) spreads more to the posterior in the distal portion of the embryo than is seen in wild type. The visceral endoderm appeared to be aberrantly displaced in mosaic embryos. There was some evidence of intermingling of visceral and definitive endoderm in lateral portions of the embryo. Consistently, we saw that the AVE extended further distally than in littermates, suggesting that it had not been displaced as normal by DE from the anterior primitive streak. This may result from some of the DE occurring more posteriorly, and thus exerting less of a displacing effect on AVE. However, by E8.0, the ventral surface of the embryo was covered by endoderm that was largely if not exclusively of epiblast origin, that is, definitive endoderm. (We cannot exclude that some of the unlabeled cells in the endoderm could be of visceral origin, but they certainly include unrecombined cells of epiblast origin.) We observed that the node was often mediolaterally expanded, at least as judged by the expression of node markers. Accordingly, it is conceivable that the anterior primitive streak (from which both DE and node derive) might also be expanded. Thus, BMPRIA signaling may have a direct role in DE formation or migration. In the mosaics, the DE tissue layer forms but the timing and distribution of its spread are abnormal.

The molecular basis of the morphogenesis pathway(s) downstream of BMPRIA is unclear. Our results demonstrate that BMP signaling through BMPRIA is required to orchestrate several aspects of germ layer morphogenesis. Given the nonautonomy of morphogenetic defects, it is likely that BMPRIA signal transduction promotes the expression or activity of a secreted factor or factors that in turn regulate the cellular behaviors underlying specific morphogenetic events. In zebrafish, BMP signaling may affect convergent-extension morphogenesis by regulating the expression of *Wnt* genes (Myers et al., 2002), which in turn encode secreted factors. The individual morphogenetic movements of early embryogenesis are very poorly understood in the mouse, but the parallels with zebrafish and other models provide hypotheses to test.

We speculate that BMPRIA signaling promotes the production of an unidentified epiblast morphogenetic signal, but we do not know its specific source or identity. Good arguments can be made for the candidacy of various Wnt, FGF, or Nodal ligands, all of which are active in establishing the body plan of the mouse embryo (reviewed by Lu et al., 2001). We are examining these factors in ongoing experiments.

BMP signaling and mediolateral regionalization of the ectoderm

The "default model" of neural induction holds that naive ectodermal cells that transduce a BMP2/4 signal will become surface ectoderm, while those that do not transduce this signal will become neural (Chang and Hemmati-Brivanlou, 1998). Consistent with this model, we observe little if any surface ectoderm rostral to the hindbrain. Instead, neurectoderm is expanded, extending to the embryonic margins. However, caudal to the hindbrain, *Bmpr1a* mosaic embryos have significant amounts of surface ectoderm, even in very strong phenotypes (though probably less than in corresponding wild-type embryos). This tissue contains cells that have undergone recombination and, therefore, presumably lack *Bmpr1a*. These data suggest that the lack of BMPRIA may inhibit the surface ectoderm fate while not precluding it. Conversely, BMPRIA activity may promote surface ectoderm formation, but is not essential for its formation.

Evidence from many experimental models suggests that BMP2/4 signaling promotes dorsal fates and inhibits ventral fates in the nascent neural plate (Lee and Jessell, 1999; Sasai and De Robertis, 1997). Indeed, zebrafish *Bmp2b/swirl* mutants show lack of neural crest, reduced dorsal neural markers, and an expanded floorplate (Barth et al., 1999;

Nguyen et al., 2000). However, in *Bmpr1a* mosaic mouse embryos, the D–V axis of the neural tube is surprisingly well patterned. Although neurulation fails at all levels, dorsal–lateral neural plate markers are not reduced, and are in some cases even expanded. Oddly, expanded domains are uneven and discontinuous, possibly related to the local degree of mosaicism in the ectoderm itself or in underlying mesoderm. Even in very strong mosaics, the neural crest is specified and can migrate away from the neural plate. Meanwhile, ventral markers are not expanded in general, with the floorplate being of essentially normal width. However, ventral regions are sometimes expanded in dysmorphic anterior regions, particularly where folds of ectoderm come near the ventral midline. This indicates that the ventralizing capacity of the axial midline is intact, but not necessarily greater than in wild-type, as one might have expected with reduced BMP signaling.

Despite the absence of what is presumed to be the key BMP2/4 type I receptor during mouse gastrulation and neurulation, we observed less severe effects on mediolateral ectodermal development than expected, given the data from *Xenopus* experiments. One possibility is that BMP signaling is indeed dispensable for surface ectoderm formation and dorsal neural patterning. Alternatively, we may have failed to sufficiently diminish BMP signaling. Recombination by Mox2-Cre may be too late, though it occurs throughout the embryo well before gastrulation begins (Tallquist and Soriano, 2000); perhaps BMPRIA is a very stable protein that persists sufficiently long. A more likely possibility is that a related receptor can transduce any required signals. *Bmpr1b* is neither expressed nor required in early mouse development (Beppu et al., 2000). Activin receptor 1A (Alk2) can bind some BMP ligands (Liu et al., 1995; Macias-Silva et al., 1998). In *Xenopus*, activated Alk2 can repress neural but promote surface ectoderm fates (Suzuki et al., 1997). In mouse, it does not appear to be required in the epiblast for development of either neural or surface ectoderm lineages (Gu et al., 1999; Mishina et al., 1999). Thus, Alk2 and BMPRIA have distinct roles in the epiblast, but may also function redundantly in neuralization. The absolute role of BMPRIA signaling in neural pattern formation must be reexamined when reagents are available to completely remove it from the epiblast.

Expanded anterior neurectoderm in Bmpr1a mosaics

A striking defect of more than 90% of the *Bmpr1a* mosaics we observed is that the neural ectoderm is expanded and convoluted from the hindbrain forward. This appears to be the expense of anterior surface ectoderm, which appeared to be absent by virtue of both morphology and a surface ectoderm gene expression marker. Though the anterior neurectoderm in mosaics occupies more surface area than in wild-type counterparts, we saw no increased proliferation in the mosaic neuroepithelium. These results suggest that the proportion of ectoderm that is neuralized is greatly increased in the anterior section of *Bmpr1a* mosaics. This is not simply a consequence of these ectodermal cells being unable to receive BMP signals, as the ‘‘neural default’’ model would suggest, because the expanded neural ectoderm was composed largely of wild-type cells in some mosaics with the expanded anterior neurectoderm phenotype (e.g., Fig. 3F).

Regional gene expression markers for A–P neural domains indicate that an expanded presumptive forebrain accounts for most of the enlarged anterior neurectoderm of *Bmpr1a* mosaics. In fact, other domains, such as midbrain and hindbrain, may even be reduced along the A–P axis relative to wild type. We suggest that these observations can best be explained by an enlarged area of presumptive anterior ectoderm being exposed to forebrain-promoting factors early in development.

Primary anterior signaling centers are expanded in Bmpr1a mosaic embryos

We observed that the prechordal plate (PrCP), residing at the rostral limit of the axial mesendoderm, was broad and often diffuses in *Bmpr1a* mosaic embryos. Exposure of mouse ectoderm explants to prechordal plate induces forebrain markers (Shimamura and Rubenstein, 1997). Because the mosaic PrCP extends laterally, it underlies a broader region of ectoderm and may influence prospective surface ectoderm toward an anterior neural fate. Consistent with this view, we observed that the PrCP sometimes failed to extend to the rostral extreme of the neurectoderm in *Bmpr1a* mosaics, exactly the region of anterior neurectoderm that shows weaker expression of forebrain markers such as *Six3*. We have found that increased BMP signaling is detrimental to the PrCP and forebrain development in mouse (Anderson et al., 2002). Thus, it is consistent that decreased BMP signal reception in *Bmpr1a* mosaics seems to enhance the influence of the widened PrCP.

We also observed that in virtually all *Bmpr1a* mosaic embryos examined at early to mid-gastrulation, the anterior visceral endoderm (AVE) was expanded. In particular, the AVE occupied a greater proportion of the A–P axis of the mosaic embryos. Increasing evidence supports the hypothesis that AVE initializes the forebrain fate (Beddington and Robertson, 1998), likely via repression of posteriorizing factors in the naive neurectoderm (Perea-Gomez et al., 2001). However, the AVE is not sufficient to induce and maintain prospective forebrain, but rather requires the synergy of organizer derivatives (Tam and Steiner, 1999). In mouse, BMP activity appears to be inhibitory to both AVE and organizer function (Bachiller et al., 2000), and a key function of the organizer (Harland and Gerhart, 1997) and possibly the AVE (Beddington and Robertson, 1998) is to inhibit BMP signaling. Therefore, with the reduced overall BMP signaling in *Bmpr1a* mosaics, the epiblast might be sensitized to the anteriorizing influence of both the AVE and the organizer.

Our data fit well with the "double assurance model" for anterior neural patterning in the mouse (Shawlot et al., 1999; Thomas and Beddington, 1996). In this scheme, forebrain fate is promoted by the AVE, but is reinforced and maintained by the anterior axial mesendoderm (e.g., PrCP). Consistent with the general point of the neural default model for initial neuralization (that reduced BMP signaling promotes a basal neural fate of anterior character), the ectoderm may be sensitized to both of these anteriorizing influences by a reduced overall level of BMP signaling in the *Bmpr1a* mosaic embryos. *Bmpr1a* mosaics have expanded AVE and PrCP, probably as a result of abnormal morphogenesis of visceral and definitive endoderm. We suggest that the expanded AVE overlies a greater extent of epiblast and induces it to a forebrain fate, thus increasing the proportion of labile forebrain in the nascent neurectoderm. Subsequently, the broad PrCP stabilizes forebrain identity in the neural ectoderm in its vicinity.

Acknowledgments

We thank B. Hogan, E. Meyers, and members of the Klingensmith lab for helpful comments on the manuscript. Plasmids were kindly provided by A. McMahon, S. Tilghman, P. Mitchell, B. Hogan. M. Tessier-Lavigne, T. Gridley, and R. Lovell-Badge. We are grateful to P. Soriano and M. Tallquist for providing Mox2-Cre mice. This work was supported by NIH awards to J.K. (R01DE013674 and P01HD39948).

References

Anderson, R.M., Lawrence, A.R., Stottmann, R.W., Bachiller, D., Klingensmith, J., 2002. Chordin and noggin promote organizing centers of forebrain development in the mouse. Development 129, 4975–4987.

Ang, S.L., Conlon, R.A., Jin, O., Rossant, J., 1994. Positive and negative signals from mesoderm regulate the expression of mouse *Otx2* in ectoderm explants. Development 120, 2979–2989.

Bachiller, D., Klingensmith, J., Kemp, C., Belo, J.A., Anderson, R.M., May, S.R., McMahon, J.A., McMahon, A.P., Harland, R.M., Rossant, J., et al., 2000. The organizer factors Chordin and Noggin are required for mouse forebrain development. Nature 403, 658–661.

Barth, K.A., Kishimoto, Y., Rohr, K.B., Seydler, C., Schulte-Merker, S., Wilson, S.W., 1999. Bmp activity establishes a gradient of positional information throughout the entire neural plate. Development 126, 4977–4987.

Beddington, R.S., Robertson, E.J., 1998. Anterior patterning in the mouse. Trends Genet. 14, 277–284.

Belo, J.A., Bouwmeester, T., Leyns, L., Kertesz, N., Gallo, M., Follettie, M., De Robertis, E.M., 1997. Cerberus-like is a secreted factor with neutralizing activity expressed in the anterior primitive endoderm of the mouse gastrula. Mech. Dev. 68, 45–57.

Beppu, H., Kawabata, M., Hamamoto, T., Chytil, A., Minowa, O., Noda, T., Miyazono, K., 2000. BMP type II receptor is required for gastrulation and early development of mouse embryos. Dev. Biol. 221, 249–258.

Camus, A., Davidson, B.P., Billiards, S., Khoo, P., Rivera-Perez, J.A., Wakamiya, M., Behringer, R.R., Tam, P.P., 2000. The morphogenetic role of midline mesendoderm and ectoderm in the development of the forebrain and the midbrain of the mouse embryo. Development 127, 1799–1813.

Chang, C., Hemmati-Brivanlou, A., 1998. Cell fate determination in embryonic ectoderm. J. Neurobiol. 36, 128–151.

Chang, H., Huylebroeck, D., Verschueren, K., Guo, Q., Matzuk, M.M., Zwijsen, A., 1999. Smad5 knockout mice die at mid-gestation due to multiple embryonic and extraembryonic defects. Development 126, 1631–1642.

Constam, D.B., Robertson, E.J., 2000. Tissue-specific requirements for the proprotein convertase furin/SPC1 during embryonic turning and heart looping. Development 127, 245–254.

Dewulf, N., Verschueren, K., Lonnoy, O., Moren, A., Grimsby, S., Vande Spiegle, K., Miyazono, K., Huylebroeck, D., ten Dijke, P., 1995. Distinct spatial and temporal expression patterns of two type I receptors for Bone Morphogenetic Proteins during mouse embryogenesis. Endocrinology 136, 2652–2663.

Downs, K.M., Davies, T., 1993. Staging of gastrulating mouse embryos by morphological landmarks in the dissecting microscope. Development 118, 1255–1266.

Dufort, D., Schwartz, L., Harpal, K., Rossant, J., 1998. The transcription factor HNF3beta is required in visceral endoderm for normal primitive streak morphogenesis. Development 125, 3015–3025.

Echelard, Y., Epstein, D.J., St-Jacques, B., Shen, L., Mohler, J., McMahon, J.A., McMahon, A.P., 1993. Sonic hedgehog, a member of a family of putative signaling molecules, is implicated in the regulation of CNS polarity. Cell 75, 1417–1430.

Fainsod, A., Steinbeisser, H., De Robertis, E.M., 1994. On the function of BMP-4 in patterning the marginal zone of the *Xenopus* embryo. EMBO J. 13, 5015–5025.

Fujiwara, T., Dehart, D.B., Sulik, K.K., Hogan, B.L., 2002. Distinct requirements for extra-embryonic and embryonic bone morphogenetic protein 4 in the formation of the node and primitive streak and coordination of left–right asymmetry in the mouse. Development 129, 4685–4696.

Gavin, B.J., McMahon, J.A., McMahon, A.P., 1990. Expression of multiple novel Wnt-1/int-1-related genes during fetal and adult mouse development. Genes Dev. 4, 2319–2332.

Glinka, A., Wu, W., Onichtchouk, D., Blumenstock, C., Niehrs, C., 1997. Head induction by simultaneous repression of Bmp and Wnt signalling in *Xenopus*. Nature 389, 517–519.

Glinka, A., Wu, W., Delius, H., Monaghan, A.P., Blumenstock, C., Niehrs, C., 1998. Dickkopf-1 is a member of a new family of secreted proteins and functions in head induction. Nature 391, 357–362.

Gu, Z., Reynolds, E.M., Song, J., Lei, H., Feijen, A., Yu, L., He, W., MacLaughlin, D.T., van den Eijnden-van Raaij, J., Donahoe, P.K., et al., 1999. The type I serine/threonine kinase receptor ActRIA (ALK2) is required for gastrulation of the mouse embryo. Development 126, 2551–2561.

Hammerschmidt, M., Mullins, M.C., 2002. Dorsoventral patterning in the zebrafish: bone morphogenetic proteins and beyond. Results Probl. Cell Differ. 40, 72–95.

Harland, R., Gerhart, J., 1997. Formation and function of Spemann's organizer. Annu. Rev. Cell Dev. Biol. 13, 611–667.

Hartley, K.O., Hardcastle, Z., Friday, R.V., Amaya, E., Papalopulu, N., 2001. Transgenic *Xenopus* embryos reveal that anterior neural development requires continued suppression of BMP signaling after gastrulation. Dev. Biol. 238, 168–184.

Hayashi, S., Lewis, P., Pevny, L., McMahon, A.P., 2002. Efficient gene modulation in mouse epiblast using a Sox2Cre transgenic mouse strain. Gene Expr. Patterns 2, 93–97.

Hogan, B.L., Beddington, R., Costantini, F., Lacy, E., 1994. Manipulating the Mouse Embryo. Cold Spring Harbor Press, New York.

Kaufman, M.H., 1992. The Atlas of Mouse Development. Academic Press, Inc., San Diego.

Kaufman, M.H., Bard, J.B.L., 1999. The Anatomical Basis of Mouse Development. Academic Press, Inc., San Diego.
Kennedy, T.E., Serafini, T., de la Torre, J.R., Tessier-Lavigne, M., 1994. Netrins are diffusible chemotropic factors for commissural axons in the embryonic spinal cord. Cell 78, 425–435.
Knecht, A.K., Bronner-Fraser, M., 2002. Induction of the neural crest: a multigene process. Nat. Rev. Genet. 3, 453–461.
Kuhlbrodt, K., Herbarth, B., Sock, E., Hermans-Borgmeyer, I., Wegner, M., 1998. Sox10, a novel transcriptional modulator in glial cells. J. Neurosci. 18, 237–250.
Lawson, K.A., Meneses, J.J., Pedersen, R.A., 1991. Clonal analysis of epiblast fate during germ layer formation in the mouse embryo. Development 113, 891–911.
Lee, K.J., Jessell, T.M., 1999. The specification of dorsal cell fates in the vertebrate central nervous system. Annu. Rev. Neurosci. 22, 261–294.
Liu, F., Ventura, F., Doody, J., Massague, J., 1995. Human type II receptor for bone morphogenic proteins (BMPs): extension of the two-kinase receptor model to the BMPs. Mol. Cell Biol. 15, 3479–3486.
Lu, C.C., Brennan, J., Robertson, E.J., 2001. From fertilization to gastrulation: axis formation in the mouse embryo. Curr. Opin. Genet. Dev. 11, 384–392.
Macias-Silva, M., Hoodless, P.A., Tang, S.J., Buchwald, M., Wrana, J.L., 1998. Specific activation of Smad1 signaling pathways by the BMP7 type I receptor, ALK2. J. Biol. Chem. 273, 25628–25636.
Mackenzie, A., Ferguson, M.W.J., Sharpe, P.T., 1991. *Hox-7* expression during murine craniofacial development. Development 113, 601–611.
Massague, J., Chen, Y.G., 2000. Controlling TGF-beta signaling. Genes Dev. 14, 627–644.
Mayor, R., Aybar, M.J., 2001. Induction and development of neural crest in *Xenopus laevis*. Cell Tissue Res. 305, 203–209.
McMahon, J.A., Takada, S., Zimmerman, L.B., Fan, C.M., Harland, R.M., McMahon, A.P., 1998. Noggin-mediated antagonism of BMP signaling is required for growth and patterning of the neural tube somite. Genes Dev. 12, 1438–1452.
Mintzer, K.A., Lee, M.A., Runke, G., Trout, J., Whitman, M., Mullins, M.C., 2001. Lost-a-fin encodes a type I BMP receptor, Alk8, acting maternally and zygotically in dorsoventral pattern formation. Development 128, 859–869.
Mishina, Y., Suzuki, A., Ueno, N., Behringer, R.R., 1995. Bmpr encodes a type I bone morphogenetic protein receptor that is essential for gastrulation during mouse embryogenesis. Genes Dev. 9, 3027–3037.
Mishina, Y., Crombie, R., Bradley, A., Behringer, R.R., 1999. Multiple roles for activin-like kinase-2 signaling during mouse embryogenesis. Dev. Biol. 213, 314–326.
Mishina, Y., Hanks, M.C., Miura, S., Tallquist, M.D., Behringer, R.R., 2002. Generation of Bmpr/Alk3 conditional knockout mice. Genesis 32, 69–72.
Mitchell, P.J., Timmons, P.M., Hebert, J.M., Rigby, P.W., Tijan, R., 1991. Transcription factor AP-2 is expressed in neural crest cell lineages during mouse embryogenesis. Genes Dev. 5, 105–119.
Miyazono, K., Kusanagi, K., Inoue, H., 2001. Divergence and convergence of TGF-beta/BMP signaling. J. Cell. Physiol. 187, 265–276.
Mullins, M.C., Hammerschmidt, M., Kane, D.A., Odenthal, J., Brand, M., van Eeden, F.J., Furutani-Seiki, M., Granato, M., Haffter, P., Heisenberg, C.P., Jiang, Y.J., Kelsh, R.N., Nusslein-Volhard, C., 1996. Genes establishing dorsoventral pattern formation in the zebrafish embryo: the ventral specifying genes. Development 123, 81–93.
Myers, D.C., Sepich, D.S., Solnica-Krezel, L., 2002. Bmp activity gradient regulates convergent extension during zebrafish gastrulation. Dev. Biol. 243, 81–98.
Nguyen, V.H., Trout, J., Connors, S.A., Andermann, P., Weinberg, E., Mullins, M.C., 2000. Dorsal and intermediate neuronal cell types of the spinal cord are established by a BMP signaling pathway. Development 127, 1209–1220.
Oliver, G., Mailhos, A., Wehr, R., Copeland, N.G., Jenkins, N.A., Gruss, P., 1995. Six3, a murine homologue of the sine oculis gene, demarcates the most anterior border of the developing neural plate and is expressed during eye development. Development 121, 4045–4055.
Pearce, J.J., Penny, G., Rossant, J., 1999. A mouse cerberus/Dan-related gene family. Dev. Biol. 209, 98–110.
Perea-Gomez, A., Rhinn, M., Ang, S.L., 2001. Role of the anterior visceral endoderm in restricting posterior signals in the mouse embryo. Int. J. Dev. Biol. 45, 311–320.
Quinlan, G.A., Williams, E.A., Tan, S.S., Tam, P.P., 1995. Neuroectodermal fate of epiblast cells in the distal region of the mouse egg cylinder: implication for body plan organization during early embryogenesis. Development 121, 87–98.
Sasai, Y., De Robertis, E.M., 1997. Ectodermal patterning in vertebrate embryos. Dev. Biol. 182, 5–20.
Sasaki, H., Hogan, B.L., 1993. Differential expression of multiple fork head related genes during gastrulation and axial pattern formation in the mouse embryo. Development 118, 47–59.
Schultheiss, T.M., Burch, J.B., Lassar, A.B., 1997. A role for bone morphogenetic proteins in the induction of cardiac myogenesis. Genes Dev. 11, 451–462.
Shawlot, W., Wakamiya, M., Kwan, K.M., Kania, A., Jessell, T.M., Behringer, R.R., 1999. Lim1 is required in both primitive streak-derived tissues and visceral endoderm for head formation in the mouse. Development 126, 4925–4932.
Shimamura, K., Rubenstein, J.L., 1997. Inductive interactions direct early regionalization of the mouse forebrain. Development 124, 2709–2718.
Soriano, P., 1999. Generalized lacZ expression with the ROSA26 Cre reporter strain. Nat. Genet. 21, 70–71.
Sulik, K., Dehart, D.B., Iangaki, T., Carson, J.L., Vrablic, T., Gesteland, K., Schoenwolf, G.C., 1994. Morphogenesis of the murine node and notochordal plate. Dev. Dyn. 201, 260–278.
Suzuki, A., Ueno, N., Hemmati-Brivanlou, A., 1997. *Xenopus* msx1 mediates epidermal induction and neural inhibition by BMP4. Development 124, 3037–3044.
Swiatek, P.J., Gridley, T., 1993. Perinatal lethality and defects in hindbrain development in mice homozygous for a targeted mutation of the zinc finger gene Krox20. Genes Dev. 7, 2071–2084.
Tallquist, M.D., Soriano, P., 2000. Epiblast-restricted Cre expression in MORE mice: a tool to distinguish embryonic vs. extra-embryonic gene function. Genesis 26, 113–115.
Tam, P.P., Steiner, K.A., 1999. Anterior patterning by synergistic activity of the early gastrula organizer and the anterior germ layer tissues of the mouse embryo. Development 126, 5171–5179.
Thomas, P., Beddington, R., 1996. Anterior primitive endoderm may be responsible for patterning the anterior neural plate in the mouse embryo. Curr. Biol. 6, 1487–1496.
Thomas, P.Q., Johnson, B.V., Rathjen, J., Rathjen, P.D., 1995. Sequence, genomic organization, and expression of the novel homeobox gene Hesx1. J. Biol. Chem. 270, 3869–3875.
Tiso, N., Filippi, A., Pauls, S., Bortolussi, M., Argenton, F., 2002. BMP signalling regulates anteroposterior endoderm patterning in zebrafish. Mech. Dev. 118, 29–37.
Waldrip, W.R., Bikoff, E.K., Hoodless, P.A., Wrana, J.L., Robertson, E.J., 1998. Smad2 signaling in extraembryonic tissues determines anterior–posterior polarity of the early mouse embryo. Cell 92, 797–808.
Wassarman, K.M., Lewandoski, M., Campbell, K., Joyner, A.L., Rubenstein, J.L.R., Martinez, S., Martin, G.R., 1997. Specification of the anterior hindbrain and establishment of a normal mid/hindbrain organizer is dependent on *Gbx2* gene function. Development 124, 2923–2934.
Weinstein, D.C., Hemmati-Brivanlou, A., 1999. Neural induction. Annu. Rev. Cell Dev. Biol. 15, 411–433.
Wilkinson, D.G., Bailes, J.A., McMahon, A.P., 1987. Expression of the proto-oncogene int-1 is restricted to specific neural cells in the developing mouse embryo. Cell 50, 79–88.
Wilkinson, D.G., Bhatt, S., Herrmann, B.G., 1990. Expression pattern of the mouse T gene and its role in mesoderm formation. Nature 343, 657–659.
Winnier, G., Blessing, M., Labosky, P.A., Hogan, B.L.M., 1995. Bone

morphogenetic protein-4 is required for mesoderm formation and patterning in the mouse. Genes Dev. 9, 2105–2116.

Wood, H.B., Episkopou, V., 1999. Comparative expression of the mouse Sox1, Sox2 and Sox3 genes from pre-gastrulation to early somite stages. Mech. Dev. 86, 197–201.

Wu, L., de Bruin, A., Saavedra, H.I., Starovic, M., Trimboli, A., Yang, Y., Opavska, J., Wilson, P., Thompson, J.C., Ostrowski, M.C., et al., 2003. Extra-embryonic function of Rb is essential for embryonic development and viability. Nature 421, 942–947.

Yi, S.E., Daluiski, A., Pederson, R., Rosen, V., Lyons, K.M., 2000. The type I BMP receptor BMPRIB is required for chondrogenesis in the mouse limb. Development 127, 621–630.

Zhao, G.Q., 2003. Consequences of knocking out BMP signaling in the mouse. Genesis 35, 43–56.